RESEARCH ARTICLE OPEN ACCESS

Design of an Ultimate High Speed Electrical Drive System

C. Vishnu Kiran, K. Puneeth Kumar, K. Vinutha
Department *of* EEE, Sree Vidyanikethan Engineering College

Abstract
New emerging applications in the areas of portable power generation, small turbocompressors and spindles require the development of ultrahigh-speed, low power electrical drives. A 500 000 r/min, 100 W electrical drive system is presented. Because of the ultrahigh-speed requirements, standard machine design and power electronic topology choices no longer apply and the complete drive system has to be considered. A permanent magnet machine with a slotless litz-wire winding is used, which results in a low motor inductance and a high fundamental machine frequency. Three different combinations of power electronic topologies and commutation strategies have been experimentally investigated. A voltage source inverter with block commutation and an additional dc–dc converter is selected as the most optimal choice for the power electronics interface as it results in the lowest volume of the entire drive system due to lower switching losses, no heat sink cooling required, a small number of semiconductor devices, and relatively simple control implementation in a low cost digital signal processor.

Index Terms—Electrical drive, high-speed, permanent magnet (PM) machine.

I. INTRODUCTION

NEW APPLICATIONS are appearing for superhigh-speed drive systems in air-compressors, spindle drives and drills [1], [2] and miniature portable power generation systems [3]. By increasing the speed, the volume of the electrical machine decreases for the same power rating, which has significant ad- vantages, especially for portable power generation. The defini- tion of superhigh-speed electrical machines is dependent on the required power level and the rated speed of the machine. Fig. 1 presents various applications and the dividing line (shown as the dashed line) between high-speed and superhigh-speed electrical machines as defined by [1]. The drives presently used in spindles and drills lie in the definition range of high-speed although there are applications emerging for superhigh-speeds. Fig. 1 also shows the application areas for turbomachinery such as industrial and microgas turbines and compressors, although only a few of these systems have a direct connection of an electrical machine. Extrapolating the turbomachinery line (dashed) predicts the operating range for ultrahigh-speed drive systems as having speeds from 400 000 to 1 000 000 r/min and power levels between 10 W and 1 kW. This paper presents a new ultrahigh-speed drive system (see Fig. 1) that is capable of operating at 500 000 r/min with a power output of 100 W for a portable power gas turbine unit and for an air-compressor ap- plication. Such a drive system presents significant challenges in terms of the design of the electrical machine power electronics interface that includes a bidirectional power capability and the drive controller.

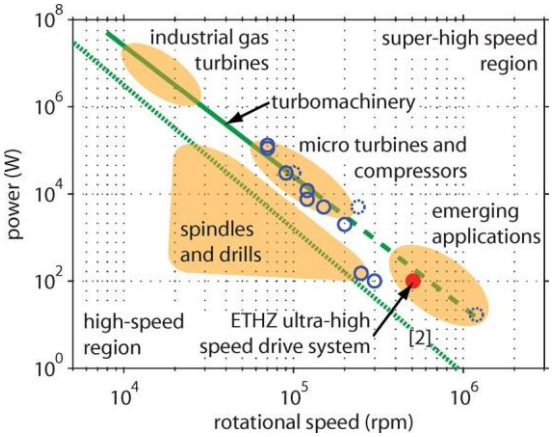

Fig. 1. Application areas and trends for superhigh-speed drive systems. Systems referenced are plotted with circles, while future trends and planned systems are given as dashed circles. The ultrahigh-speed drive for a portable power application, as described in this paper, is highlighted.

Power levels between 10 W and 1 kW. This paper presents a new ultrahigh-speed drive system (see Fig. 1) that is capable of operating at 500 000 r/min with a power output of 100 W for a portable power gas turbine unit and for an air-compressor ap- plication. Such a drive system presents significant challenges in terms of the design of the electrical machine power electronics interface that includes a bidirectional power capability and the drive controller.

Fig. 1 presents the turbomachinery trend line starting from industrial gas-turbines in the megawatt power range, then extends down to microgas turbines

with tens of kilowatt of power and finally is projected to research projects with power outputs of 10 to 100 W. For the industrial gas turbines, the grid-connected generator is coupled to the turbine through a gearbox and operates at a lower speed. Microgas turbines that have direct connected high-speed permanent magnet (PM) generators/starters delivering 10 to 100 kW are becoming more prevalent [4], [5]. For example, the Capstone microgas turbine operates at 90 000 r/min with a power output of 30 kW [6]. Several international research groups are investigating ultrami- crogas turbines with power outputs of up to 100 W for use in portable power applications [3], [7], [8]. Only a few of these projects consider the electrical system, although the electrical drive system is an integral part of the total system to start and generate electrical power from the turbines.

For compressor systems, the power and speed trends are similar to the turbines. One application is a fuel cell air com- pressor that requires 120 000 r/min at 12 kW [9] and another is a 70 000 r/min, 131 kW turbo compressor connected to a PM machine and inverter [10]. Future automotive fuel cells will require low power compressors which are small and lightweight and directly driven by high-speed electrical drives.

The present spindle drives mainly use induction motors [11], but a significant number are being replaced by PM machines due to higher efficiency and power density, especially since the speed range extends up to 250 000 r/min with a constant power of approximately 100 W [12]. The trend to smaller, higher precision work pieces, together with higher productivity requirements and smaller drill holes, will facilitate the develop- ment of ultrahigh-speed electrical drive systems.

Emerging application areas exist for air compressors, ul- trasmall drills and spindles, and portable power generation produced by mesoscale gas-turbines. All these applications require a low power, ultrahigh-speed electrical drive system. In this paper, a 500 000 r/min, 100-W motor/generator drive system that can be coupled directly to a gas turbine is presented. In Section II, the complete drive system is discussed because the machine, power electronics interface and control cannot be treated in isolation. Section III describes the PM machine construction and the resulting electrical parameters. Since the designed machine has a high fundamental frequency and low inductance, the standard voltage source inverter (VSI) cannot be assumed to be the optimal choice. In Section IV, the converter topology selection, commutation strategy and position sensing methods are discussed. Experimental verification of the three topology and commutation strategy combinations and the final drive system implemented with a VSI with block commutation are presented in Section V.

II. DRIVE SYSTEM OVERVIEW

The main application is for a portable power unit where the output is used to power portable electronic devices of up to 100 W. The output voltage is specified as dc with a voltage range from 28 to 42 V as this level enables it to be utilized in both aircraft and automotive electrical systems. For most applications, the requirements are a small size, high efficiency, and simple control structure since high dynamical control of the torque or speed is not required.

For the emerging applications that require ultrahigh-speeds at low output powers, new electrical drive systems need to be de- veloped where both the machine and power electronics designs are considered together. The application, either as the driving source and/or load, must be considered because mechanical couplings between the systems are not feasible. The machine selection and construction influence the power electronics and the use of standard rotor angle position sensors are no longer feasible.

To achieve a small size for the overall system, all the components in the system must be considered. The electrical machine scales with torque and the machine type, where for smaller machines the torque to volume ratio becomes smaller. At the rated speed, only a brushless machine can be used due to low frictional losses. For the power electronics converter, the size is dependent on the power, power losses, topology and passive components. The control electronics scale with control

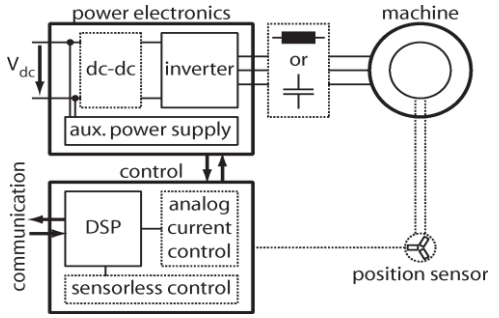

Fig. 2. Block diagram of the ultrahigh-speed drive system. Necessary systems are drawn as solid lines, while topology dependent parts are shown with dashed lines.

complexity and the level of functionality integration. At the 100 W power level, the power electronics and electrical ma- chine will be rather small, but control electronics can become large depending on the topology, commutation strategy and po- sition detection system. Therefore, reducing control complexity is also important.

Fig. 2 shows the overall block diagram of the drive sys- tem. The electrical machine is selected as a PM machine (Section III). The main function of power

electronics is to form ac currents for the machine and to allow for bidirectional power flow. Depending on the inverter topology and commutation strategy implemented, an additional dc–dc converter or fast analog current control may be required. This is also valid for the external passive components, where external inductors are required for a high-frequency VSI or external capacitors are required for a current source inverter (CSI). The drive control is implemented in a digital signal processor (DSP) and this allows the drive to communicate with other control systems. An additional auxiliary power supply is required for the gate drivers, DSP and other control electronics. For control of the drive, either a position sensor or sensorless control has to be implemented in hardware and/or software on the control platform. The choice and design of the electrical machine is now considered, followed by the consideration of the various power electronic topologies and the control system options.

III. ELECTRICAL MACHINE DESIGN

The main challenges in the design of the electrical machine are the losses due to the high frequency in the stator core and windings, the rotor dynamics and a rotor design that minimizes the mechanical stresses and eccentricity. A PM machine is chosen with the aim of a low system volume, since PM flux density remains constant for decreasing machine volume. In contrast, the flux density in an electrically excited motor de- creases with decreasing size and is therefore not suitable for this application. High-speed operation requires a simple and robust rotor geometry and construction, and excessive mechanical stresses can be limited with a small rotor diameter. Therefore, a radial-flux machine is selected with a cylindrical PM encased in a titanium retaining sleeve. A length-to-diameter ratio of 1 : 1 is defined as this leads to a short shaft which increases the critical speeds. For the highest torque density, high-energy rare Earth

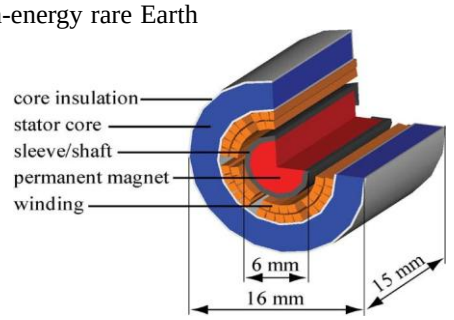

Fig. 3. Cross section of the slotless brushless PM generator. The machine has a total volume of 3.5 cm^3.

TABLE I
SPECIFICATIONS OF THE PM MACHINE

Connection	Y	
Number of pole pairs	np	1
Rated current	In	3 A
Rated frequency	fn	8.3 kHz
Rated power	Pn	100 W
Rated Torque	Tn	2 mNm
Stator resistance	Rs	0.13 Ω
Stator inductance	Ls	6.2 µH
Magnet flux linkage	ψ_m	0.31 mVs

magnets such as sintered NdFeB or SmCo are the only choices. A Sm_2Co_{17} based magnet is chosen because of its outstand- ing thermal characteristics with operating temperatures up to 350 °C. A new self-supporting, slotless litz-wire winding is used to keep the rotor losses low and the stator core manufac- turing simple [13]. The large air gap due to the ironless rotor and slotless winding results in a very low winding inductance of 6.2 μH. The peak value of the back electromotive force (EMF) is set to 16 V to allow the use of low on-resistance power MOSFETs in the power electronic converter and fulfill the specifications of operating from a low voltage dc bus.

The diametrically magnetized, cylindrical PM leads to a sinusoidal back EMF. The PM has only two poles to keep the fundamental frequency low. Nevertheless, the frequency of the currents and the magnetic field in stator winding and core reaches 8.3 kHz at rated speed. This leads to high eddy-current and hysteresis losses. The copper losses are minimized with a litz-wire winding. Compared to a standard winding the copper loss is reduced by 70%. The stator is manufactured from high frequency silicon steel; however, the iron losses outweigh the copper losses and therefore new magnetic materials such as amorphous or nanocrystalline-iron-based materials are being investigated.

The machine has an active length of 15 mm and a stator di- ameter of 16 mm. A cross section representation of the machine is shown in Fig. 3 and the nominal values and parameters of the machine are given in Table I. A detailed electromagnetic and mechanical design description is presented in [14], the test bench setup and measurement results are shown in [15] and the machine is optimized for efficiency in [16].
For machinery with speeds in the range of 500 000 r/min, the selection of a suitable bearing is the main issue. The choice is

Fig. 4. Photograph of the stator and rotor of the drive system. The extra long titanium rotor, containing two magnets, is used for a motor–generator test bench. A high-speed ball bearing is mounted on each end of the rotor.

influenced by the operating conditions and design limitations such as required stiffness, operating temperatures, atmosphere, allowed volume, and lifetime. These factors are very much dependent on the application, and usually the bearing is consid- ered as part of the application, therefore the possible choices are only compiled and briefly compared and no recommendation is given.

High-speed ball bearings are commonly used in the den- tal industry, and bearings are available for speeds exceeding 500 000 r/min. The main advantages of ball bearings are the ro- bustness and small size. The main disadvantages are the limited operating temperature and a lifetime dependent on lubrication, load and speed.

Static air bearings, dynamic air bearings, and **foil bear- ings** levitate the rotor with air pressure, either generated with an external supply (static) or by spinning the rotor (dynamic and foil). These bearings all show low friction losses and a long life-time. Foil bearings are reported for speeds up to 700 000 r/min and temperatures up to 650 ˚C [17], but are not commercially available and require a complex design procedure.

Magnetic bearings levitate the rotor using magnetic forces and have similar advantages to air bearings. However, active magnetic bearings require sensors, actuators and control, which results in high complexity and an increased bearing volume.

In summary, all bearings apart from ball bearings have no wear and just air friction and therefore a long lifetime and low losses. Because of their simplicity, robustness, small size and avoidance of auxiliary equipment, ball bearings are selected for the initial motor–generator test bench. Since a mechanical coupling at these speeds is not feasible, an overlong rotor con-taining two magnets, one for a motor and one for a generator, is supported by two high-speed ball bearings. A stator and the rotor (for the test bench) are shown in Fig. 4.

IV. POWER ELECTRONICS SELECTION AND OPERATION

The very high fundamental frequency and low motor in- ductance, coupled with the requirement for a small and light- weight design, present significant design challenges for the power electronics interface. The requirements depend on the application; however, for most of them, a compact size and low weight is needed, and also because at these speeds the

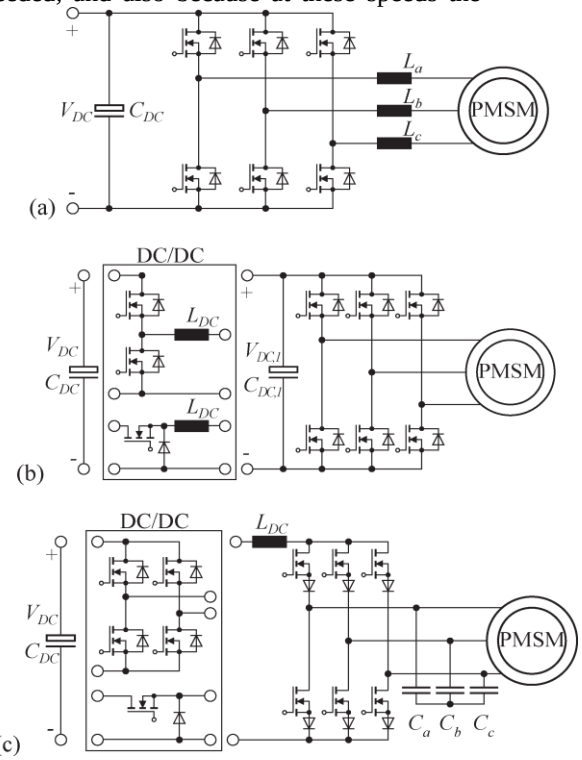

Fig. 5. Possible Power Electronic Interfaces: (a) VSI with external induc- tances, (b) VSI for block commutation and (c) CSI with external capacitors. Switching at fundamental frequency (8.3 kHz) the VSI (b) and CSI (c) need an additional dc–dc converter, either (top) bidirectional for motor and generator operation or (bottom) unidirectional for motor only operation.

electronics tend to be bigger than the machine itself. There are several possible converter topologies for connecting a dc voltage bus to a three-phase machine. To select a suitable topology and commutation strategy, both the converter and the machine have to be considered in terms of losses, number of additional passive components and method of rotor position and speed sensing. In all the applications, there is no need for high dynamics in speed control or even position control, and therefore sensorless position estimation is desirable because in most applications there are space restrictions, especially in the axial direction where a position sensor is usually placed. This section first

compares three different combinations of converter topology and commutation strategies and then compares differ- ent methods of position sensing.

4.1 .Converter Topologies and Commutation Strategies

For PM synchronous machines (PMSM) and brushless dc (BLDC) motors, VSIs are typically used, as shown in Fig. 5(a). The phase currents of the machine can be controlled to form sine (PMSM drive system) or square waves (BLDC drive sys- tem). The former has the advantage of no torque ripple due to the sinusoidal back EMF waveform, but only the BLDC control method is considered in this paper as it has a much lower control complexity and is better suited for simple sensorless control, especially at high-speeds.

For the BLDC drive system, the usual power electronic inter- face is a VSI working in chopper operation. Each phase current is controlled with a hysteresis band controller that switches the corresponding phase leg for 120 electrical degrees. This means that the switching frequency of the controlled phase leg has to be at least an order of magnitude higher than the fundamental frequency. For this ultrahigh-speed drive system, this results in switching frequencies exceeding 200 kHz, which requires a very high current control loop bandwidth and leads to high switching losses. The switching frequency also depends on the dc voltage, the hysteresis bandwidth and the machine phase inductance. For this commutation scheme, the control effort is relatively high with three current measurements needed, a comparator for hysteresis control and logic circuits for com- bining the digital control and analog signals. The very small machine inductance is a disadvantage for this commutation strategy because it leads to excessive switching frequencies and therefore external phase inductors have to be added to lower the switching frequency or current ripple.

Because of these drawbacks, inverters switching at the funda- mental frequency of the machine become attractive at ultrahigh- speeds. If a controlled dc voltage is supplied to the VSI, the VSI can then be switched at the fundamental frequency of the machine, which is commonly known as block commutation. For VSIs operating with block commutation, the small motor inductance is an advantage because there is a short current commutation time and no external phase inductors are required. The drawback is that an additional uni- or bidirectional dc–dc converter is needed to control the input dc voltage to the VSI [Fig. 5(b)]. The dc–dc converter can be designed for low volumes by increasing the switching frequency and therefore decreasing the dc inductor. The phase currents cannot be con- trolled directly as they are dependent on the machine inductance and resistance, the back EMF and the dc–dc output voltage. In steady state, the phase currents are directly proportional to the dc current.

The second topology that can be switched at fundamental frequency is the CSI as shown in Fig. 5(c). For this topology, decoupling capacitors are required on the three-phase output, and an additional dc–dc converter is needed to control the dc current level. The CSI has a unidirectional current flow and therefore needs an additional full bridge converter to change the polarity of the input voltage for bidirectional power flow. For unidirectional power flow, a buck converter is sufficient. For this topology, a small machine inductance is also an advantage. Nevertheless, a small inductance together with the decoupling capacitors leads to oscillations which have to be damped.

Figs. 6–8 present the Simulink/Matlab with PLECS sim- ulation waveforms from each of the three power electronic interfaces; the VSI with external inductors [Fig. 5(a)], VSI with block commutation [Fig. 5(b)] and CSI [Fig. 5(c)], respectively. The machine has been modeled using the parameters specified in Table I. For all topologies, the waveforms that are plotted are the back EMF (used as the reference), one-phase current, the switching signals of the corresponding phase leg and the phase voltage (machine terminals to externally reproduced star point).

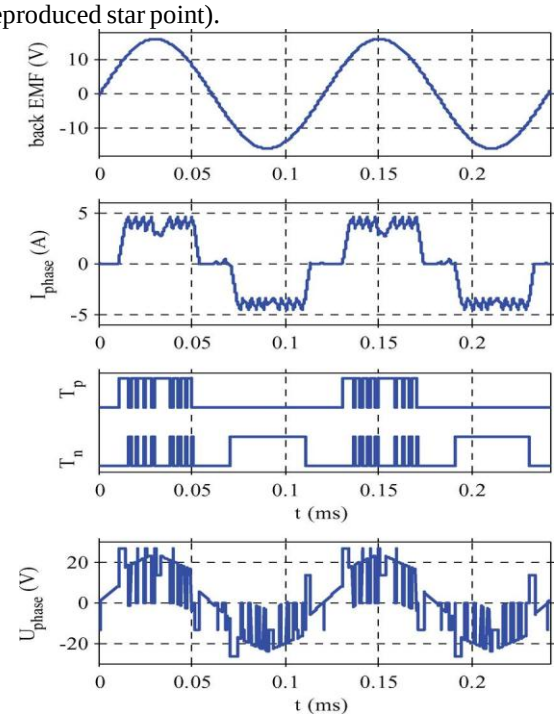

Fig. 6. Simulation of the drive system at 500 000 r/min with a VSI and additional external inductances ($L_a = L_b = L_c = 10\ \mu H$, $V_{DC} = 40$ V). Machine back EMF, phase current, half-bridge switching signals and phase voltage for one phase are shown. The switching frequency is approximately $f_s = 230$ kHz.

All the converters operate from a 35-V dc bus and deliver an electrical power of 100 W to the machine.

For the VSI with external inductors of 10 μH, the waveforms

in Fig. 6 show that the current ripple is still 1 A for a phase current of 4 A even with a switching frequency of 230 kHz. The terminal voltage of the machine also exhibits the high frequency switching and this can make sensorless position control difficult as discussed in the next section.

Fig. 7 shows the waveforms produced when a VSI with block commutation is used. The dc–dc converter at the VSI input controls the phase current to be on average 4 A. The low switching frequency can be clearly seen as well as the small commutation time. The waveforms of the CSI block commutation topology are presented in Fig. 8. Here, the phase current is well controlled compared to the VSI implementation, although there are large oscillations in the terminal voltage due to the *LC* circuit formed by the motor inductance and the decoupling capacitors.

4.2. Position Detection

Synchronous PM motor drives require rotor position infor- mation to provide the proper commutation sequence of the phase currents. There is the possibility of mechanical, optical or magnetic position sensors. Mechanical sensors are speed limited and resolvers need a large volume considering the extra

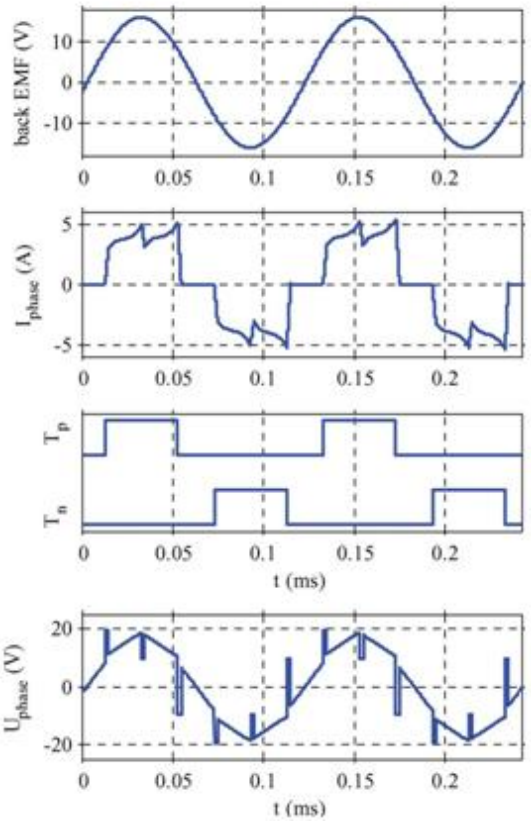

Fig. 7. Simulation of the drive system at 500 000 r/min with a VSI with block commutation an additional dc–dc converter (f_{dcdc} = 100 kHz, L_{dcdc} = 50 μH). Machine back EMF, phase current, half-bridge switching signals and phase voltage for one phase are shown. The inverter switching frequency is the fundamental frequency of the machine (8.3 kHz).

electronics needed. Therefore, only Hall sensors are an option for a compact ultrahigh-speed drive system, but they require an axial extension of the machine and may need an extra magnet in the rotor to provide a field for the sensors. Furthermore, they are temperature sensitive, and are limited to an operating temperature of 100 ˚C. Mounting inaccuracies of the sensors cause the switching instants to be displaced from the ideal position. Therefore, sensorless control is the preferred choice for this ultrahigh-speed drive system.

For BLDC drives, several sensorless control strategies exist, most of them based on back EMF estimation or measurement [18]. One of the simplest, which requires no current sensors and no DSP computation time, uses a small electronic circuit to determine the zero crossing of the back EMF [19]. In the nonen- ergized phase of the machine, the back EMF can be measured, which, for currents in phase with voltages, should cross zero in the 60 electrical degree interval of zero current. This position information can be used to commutate the currents 30 electrical degrees later. For high frequency operation of the VSI, it can be seen (Fig.

6, U_{phase}) that this method needs additional filtering or more complex algorithms to extract the position information. There exist several strategies such as back EMF integration [20] or third harmonic detection [21]. For block commutation of the VSI the back EMF zero crossing can be measured without filtering. Only during commutation of a current from one phase to the next, where the one diode of the previously active

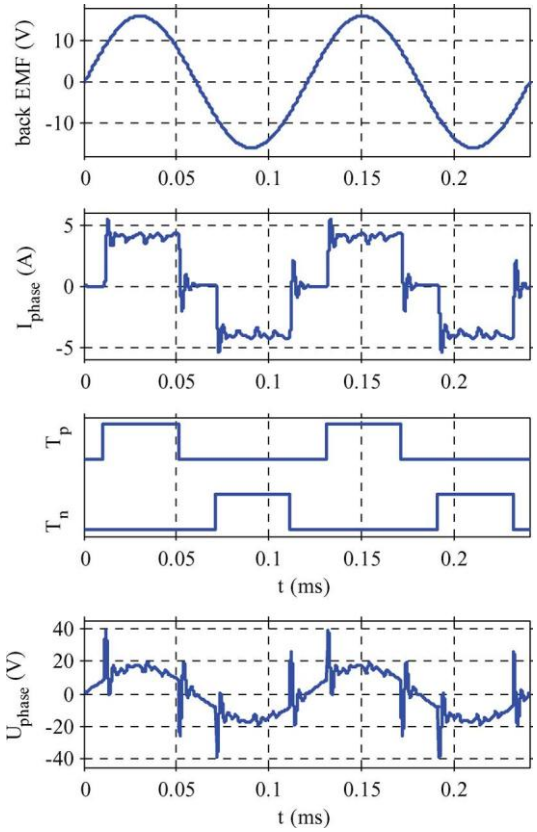

Fig. 8. Simulation of the drive system at 500 000 r/min with a CSI with block commutation an additional dc–dc converter (f_{dcdc} = 100 kHz, L_{dcdc} = 100 μH). Machine back EMF, phase current, half-bridge switching signals and phase voltage for one phase are shown. The inverter switching frequency is the fundamental frequency of the machine (8.3 kHz).

phase leg is conducting, the measured phase voltage (Fig. 7, U_{phase}) cannot be used. This time can be calculated knowing the inductance of the machine and be accounted for in a digital controller. For this commutation and sensorless control strategy, the machine has to have a small inductance such that the diode conduction angle is significantly less than 30 electrical degrees [22]. This requirement is fulfilled in the previously described machine since it is designed with a slotless winding and ironless rotor. The CSI with block commutation also allows for rela- tively easy sensing of the phase voltages although additional filtering is required in the terminal voltage signals due to the oscillations after the switching instants (Fig. 8, U_{phase}).

4.3. Power Electronics Interface

The small machine inductance is an advantage for CSI (easy decoupling of the phase and dc current) and the VSI with block commutation (short current commutation angle). The small inductance is a disadvantage for the standard VSI operation because external inductors are required to limit the switching frequency. The VSI with block commutation has an advantage because sensorless control can be realized with simple back EMF zero crossing detection without filtering. The selection of the suitable topology and commutation strategy depends on the acceptable tradeoffs between topology complexity, commu- tation and control complexity, and position detection method.

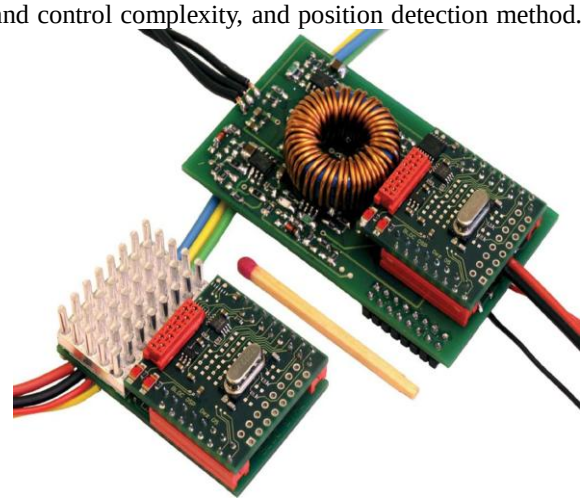

Fig. 9. Photograph of the power electronics interfaces: (top) CSI and (bottom) VSI, making use of the same digital control board. Including the auxiliary power supply and the external inductors, the VSI volume is comparable.

For the 500 000 r/min, 100 W application, the VSI with block commutation and sensorless control has the most advantages.

The realized hardware for the VSI and CSI can be seen in Fig. 9. The CSI circuit board is shown at the top of the photograph. The dc inductor is a predominant feature on the circuit board. The standard VSI is the bottom circuit board. This VSI does not have the external inductors or the additional dc–dc converter required for block commutation operation. When the external inductors or dc–dc converter are considered, the size of the total converter and control electronics is similar to that of the CSI.

The control of the machine in all cases is implemented dig- itally with a low-cost DSP from Microchip (the small plug-on board on top of the main power board). The dc–dc converter on the CSI board operates with a high switching frequency in order to use a

small inductor. Phase current measurements are imple- mented with a low value resistive shunt and amplified using an op-amp, and the sampling of the currents is synchronized with the switching. The power switches are DirectFET MOSFETs and the isolated gate drive is provided by an integrated half- bridge driver IC.

V. DRIVE SYSTEM EVALUATION

A test bench has been constructed to experimentally verify the performance of the different power electronic interfaces [15]. Two machines, as described in Section III, are arranged on a common shaft since a mechanical coupling is not feasible at the rated speed. The shaft is supported by two radial single row high-speed ball bearings and contains two PMs, one for each machine, to form the rotor. One machine is operated as the driving motor with the power electronic interfaces described in Section IV, and the other as the generator with a three-phase resistive load.

Fig. 10(a) shows the waveforms for one-phase current, the switching signals of the corresponding phase leg and the measured phase voltage when the VSI with hysteresis current control is used. The rotor position information is obtained by measuring the stray rotor field with hall switches at the end of

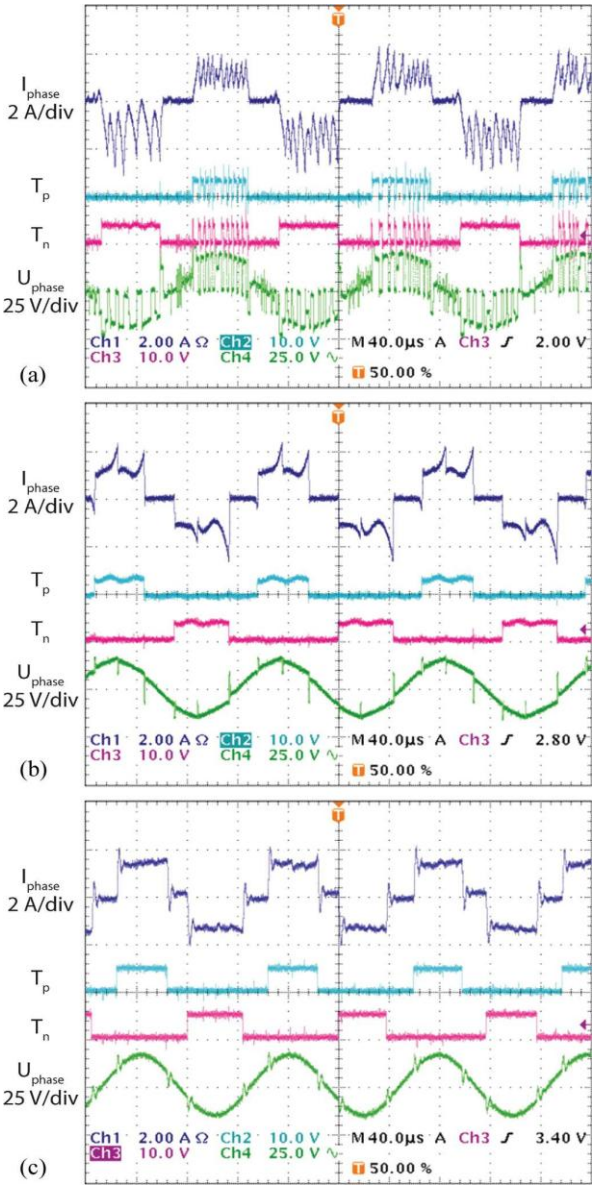

Fig. 10. Experimentally measured phase current, switching signals and ma- chine terminal phase voltage for (a) the VSI with hysteresis current control, (b) VSI with block commutation and controlled dc input voltage, (c) CSI with block commutation and controlled dc input current. The drive system is operating at 500 000 r/min, the generator is running at no load, and the controller is using Hall position sensors.

the machine. The drive system is operating at 500 000 r/min and the generator is running at no load. It can be seen that the switching frequency is approximately 230 kHz and the current ripple is large at between 1 and 2 A. Optimization of the current measurement and hysteresis controller is difficult to achieve due to the high frequency switching noise, misalignment in the position sensors and delay in the control loop. Furthermore, during the off interval of the phase leg (both switches open), a rotor position error can result in conduction

of the lower diode. This leads to spikes in the measured phase voltage, which in reality look more distorted in the off interval compared to the simulations. Therefore, the zero crossing detection for sensorless control is difficult to realize.

In the measurements for the VSI with block commuta- tion, the phase current differs slightly from the simulations [Fig. 10(b)]. This asymmetry is due to the misalignment of the switching instants resulting from mounting inaccuracies of the Hall sensors. Since the current waveform depends directly on the back EMF, a sensorless control implementation based on back EMF zero crossing detection would solve this problem. The measured phase voltage looks as in the simulations and therefore sensorless control is feasible for this topology.

In Fig. 10(c), the same measured waveforms are shown for the CSI with block commutation. The phase current oscillations are damped more effectively than in the simulations. This is due to additional parasitic resistances such as the high-frequency core losses in the stator and resistive drops in the cabling and connectors. The lower level oscillations in the measured phase voltage provide an advantage for sensorless control since the exact zero crossing of the back EMF can be detected by using a small phase voltage filter. This is an improvement compared to the results obtained by simulations.

The experiments show that all converters are feasible for speeds up to 500 000 r/min. The VSI with hysteresis controller needs the most hardware effort due to the analog current control, needs a proper tuning of the current control, and is the most sensitive to misalignment of the Hall sensors and current measurement noise. The VSI and CSI with block commuta- tion have similar hardware effort and the same low control effort. They are not limited in driving the machine with even higher speeds and in an overspeed test a maximum speed of 600 000 r/min has been achieved with the CSI.

From the experimental verification of the three power elec- tronic interfaces, the VSI with block commutation is selected as the best because it has the lowest volume of the entire drive system. This choice allows simple sensorless control to be implemented, the speed not limited due to limited switching frequency as for normal VSI, no heat sink cooling is required due to fundamental frequency operation and low switching losses, and it uses fewer semiconductor components than the CSI but has a similar performance. The sensorless speed control and dc–dc converter control can be implemented in a low cost DSP. The power electronics interface, DSP controller, motor stator and rotor are shown together in Fig. 11. As can been seen, the combined power electronics interface and controller are larger than the machine.

The major challenge for the future application of the ultrahigh-speed drive is finding an improvement in bearing technology. The present bearings have a limited lifetime at an operating speed of 500 000 r/min. To achieve higher speeds and lower frictional losses, the use of air, magnetic or hybrid bearings are being investigated. It is planned to redesign the drive system such that a speed of 1 000 000 r/min at 100 W output is achieved, and to increase the output power of 1 kW at a speed of 500 000 r/min.

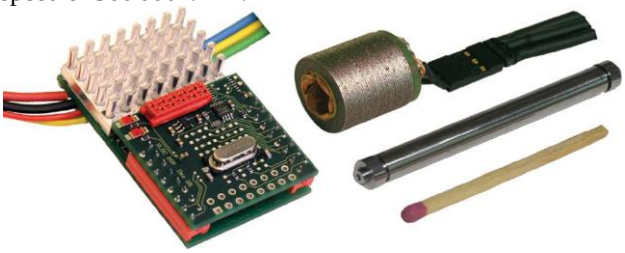

Fig. 11. Photograph of the power electronics interface (VSI) and motor stator and rotor.

VI. CONCLUSION

New emerging applications in the areas of portable power generation, small turbo compressors and spindles require the development of ultrahigh-speed, low power electrical drives. A 500 000-r/min, 100-W electrical drive system has been de- veloped. Because of the ultrahigh-speed requirements, stan-dard machine design and power electronic topology choices no longer apply and the complete drive system has to be considered.

A PM, two-pole machine with a slotless litz-wire winding has been constructed which has high efficiency, high power density, and a simple mechanical construction. To achieve a small diameter rotor, the PM is placed inside a titanium sleeve. The large air-gap results in a low motor inductance of 6.2 μH and the high operating speed means the fundamental machine frequency is 8.3 kHz. Therefore, a standard VSI implemen- tation is not an automatic choice for the power electronics interface.

Three different combinations of power electronic topologies and commutation strategies have been experimentally investi- gated. For this 500 000-r/min, 100-W application, a VSI with block commutation and an additional dc–dc converter is se-lected as the most optimal choice as it results in the lowest volume of the entire drive system due to the low switching losses, no heat sink cooling, small number of semiconductor devices, and relatively simple control implementation in a low cost DSP. Rotor position detection can be implemented in a sensorless method by using zero crossing detection of back EMF. The complete drive system concept can be

extended to higher speeds or power levels with an improvement in bearing technology and this will result in new application areas.

REFERENCES

[1] M. A. Rahman, A. Chiba, and T. Fukao, "Super high speed electrical machines—Summary," in *Proc. IEEE Power Eng. Soc. General Meeting*, Jun. 6–10, 2004, vol. 2, pp. 1272–1275.

[2] J. W. Kolar, C. Zwyssig, and S. D. Round, "Beyond 1 000 000 rpm—Review of research on mega-speed drive systems," in *Proc. COBEP*, Blumenau, Brazil, Sep. 30–Oct. 4, 2007.

[3] S. A. Jacobson and A. H. Epstein, "An informal survey of power MEMS," in *Proc. ISMME*, Tsuchiura, Japan, Dec. 1–3, 2003, pp. 513–520.

[4] O. Aglén, "Loss calculation and thermal analysis of a high-speed genera- tor," in *Proc. IEEE Int. Elect. Mach. Drives Conf.*, Jun. 1–4, 2003, vol. 2, pp. 1117–1125.

[5] J. Oyama, T. Higuchi, T. Abe, K. Shigematm, X. Yang, and E. Matsuo, "A trial production of small size ultra-high speed drive system," in *Proc. IEMDC*, 2003, vol. 1, pp. 31–36.

[6] *Capstone C30 Product Datasheet*. [Online]. Available: http://www. microturbine.com

[7] B. Schneider, M. Bruderer, D. Dyntar, C. Zwyssig, M. Diener, K. Boulouchos, R. S. Abhari, L. Guzzella, and J. W. Kolar, "Ultra-high- energy-density converter for portable power," in *Proc. 5th Int. Workshop Micro Nanotechnology for Power Generation Energy Convers. Appl.*, Tokyo, Japan, Nov. 28–30, 2005, pp. 81–84.

[8] A. H. Epstein, "Millimeter-scale, MEMS gas turbine engines," presented at the Proc. ASME Turbo Expo, Power for Land, Sea, and Air, Atlanta, GA, Jun. 16–19, 2003, Paper GT2003-38866.

[9] MiTi Developments, *Oil-Free, Motorized, Automotive Fuel Cell Air Compressor/Expander System*, Nov. 2005. [Online]. Available: http://www.miti.cc

[10] B. H. Bae, S. K. Sul, J. H. Kwon, and J. S. Byeon, "Implementation of sen- sorless vector control for super-high-speed PMSM of turbo-compressor," *IEEE Trans. Ind. Appl.*, vol. 39, no. 3, pp. 811–818, May/Jun. 2003.

[11] A. Boglietti, P. Ferraris, M. Lazzari, and F. Profumo, "About the design of very high frequency induction motors for spindle applications," in *Conf. Rec. IAS Annu. Meeting*, 1992, pp. 25–32.

[12] *Westwind D1733—250 000 rpm PCB Drilling Spindle*. [Online]. Available: http://www.westwind-airbearings.com

[13] N. Bianchi, S. Bolognani, and F. Luise, "Potentials and limits of high- speed PM motors," *IEEE Trans. Ind. Appl.*, vol. 40, no. 6, pp. 1570–1578, Nov./Dec. 2004.

[14] C. Zwyssig, J. W. Kolar, W. Thaler, and M. Vohrer, "Design of a 100 W, 500 000 rpm permanent-magnet generator for mesoscale gas turbines," in *40th Conf. Rec. IAS Annu. Meeting*, Hong Kong, Oct. 2–6, 2005, vol. 1, pp. 253–260.

[15] C. Zwyssig, S. D. Round, and J. W. Kolar, "Analytical and experimental investigation of a low torque, ultra-high speed drive system," in *Conf. Rec. IAS Annu. Meeting*, Tampa, FL, Oct. 8–12, 2006, vol. 3, pp. 1507–1513.

[16] J. Luomi, C. Zwyssig, A. Looser, and J. W. Kolar, "Efficiency optimiza- tion of a 100-W, 500 000-rpm permanent-magnet machine including air friction losses," in *Conf. Rec. IAS Annu. Meeting*, New Orleans, LA, 2007, pp. 861–868.

[17] M. Salehi, H. Heshmat, J. F. Walton, II, and M. Tomaszewski, "Operation of a mesoscopic gas turbine simulator at speeds in excess of 700 000 rpm on foil bearings," presented at the ASME Turbo Expo, Power for Land, Sea, and Air, Vienna, Austria, Jun. 14–17, 2004, Paper GT2004-53870.

[18] P. P. Acarnley and J. F. Watson, "A review of position sensorless operation of brushless permanent-magnet machines," *IEEE Trans. Ind. Electron.*, vol. 53, no. 2, pp. 352–362, Apr. 2006.

[19] K. Rajashekara, A. Kawamura, and K. Matsuse, "Position sensorless control of permanent magnet AC motors," in *Sensorless Control of AC Motor Drives*. Piscataway, NJ: IEEE Press, 1996.

[20] R. C. Becerra, T. M. Jahns, and M. Ehsani, "Four quadrant sensorless brushless ECM drive," in *Proc. IEEE Appl. Power Electron. Conf. Expo.*, 1991, pp. 202–209.

[21] J. C. Moreira, "Indirect sensing for rotor flux position of permanent magnet AC motors operating in a wide speed range," in *Conf. Rec. IAS Annu. Meeting*, 1994, pp. 401–407.

[22] Z. Q. Zhu, J. D. Ede, and D. Howe, "Design criteria for brushless DC motors for high-speed sensorless operation," *Int. J. Appl. Electromagn. Mech.*, vol. 15, no. 1–4, pp. 79–87, 2001/2002.